



Medium resolution near-infrared spectra of the host galaxies of nearby quasars

Huynh Anh Nguyen Le^a, Soojong Pak^{a,*}, Myungshin Im^b, Minjin Kim^c,
Chae Kyung Sim^a, Luis C. Ho^{d,e}

^a School of Space Research, Kyung Hee University, 1732 Deogyong-daero, Giheung-gu, Yongin-si, Gyeonggi-do 446-701, Republic of Korea

^b Department of Physics and Astronomy, Seoul National University, Center for the Exploration of the Origin of the Universe (CEO), Seoul, Republic of Korea

^c Korea Astronomy and Space Science Institute, Daejeon, Republic of Korea

^d Kavli Institute for Astronomy and Astrophysics, Peking University, Beijing 100871, China

^e Department of Astronomy, Peking University, Beijing 100871, China

Received 13 January 2014; received in revised form 20 May 2014; accepted 21 May 2014

Available online 3 June 2014

Abstract

We present medium resolution near-infrared host galaxy spectra of low redshift quasars, PG 0844 + 349 ($z = 0.064$), PG 1226 + 023 ($z = 0.158$), and PG 1426 + 015 ($z = 0.086$). The observations were done by using the Infrared Camera and Spectrograph (IRCS) at the Subaru 8.2 m telescope. The full width at half maximum of the point spread function was about 0.3 arcsec by operations of an adaptive optics system, which can effectively resolve the quasar spectra from the host galaxy spectra. We spent up to several hours per target and developed data reduction methods to reduce the systematic noises of the telluric emissions and absorptions. From the obtained spectra, we identified absorption features of Mg I (1.503 μm), Si I (1.589 μm) and CO (6-3) (1.619 μm), and measured the velocity dispersions of PG 0844 + 349 to be $132 \pm 110 \text{ km s}^{-1}$ and PG 1426 + 015 to be $264 \pm 215 \text{ km s}^{-1}$. By using an $M_{\text{BH}}-\sigma$ relation of elliptical galaxies, we derived the black hole (BH) mass of PG 0844 + 349, $\log(M_{\text{BH}}/M_{\odot}) = 7.7 \pm 5.5$ and PG 1426 + 015, $\log(M_{\text{BH}}/M_{\odot}) = 9.0 \pm 7.5$. These values are consistent with the BH mass values from broad emission lines with an assumption of a virial factor of 5.5.

© 2014 COSPAR. Published by Elsevier Ltd. All rights reserved.

Keywords: Galaxies; Active-galaxies; Kinematics and dynamics

1. Introduction

Nearby galaxies have bulge with supermassive black holes (Richstone et al., 1998). Understanding the link between the supermassive black holes and their host galaxies is important in studying the formation and evolution of the galaxies. The relation of $M_{\text{BH}}-\sigma$ has been discovered, in which M_{BH} is the mass of supermassive black hole and σ is

the stellar velocity dispersion of the bulge (e.g., Ferrarese et al., 2001; Gebhardt et al., 2000a; Gebhardt et al., 2000b).

Nevertheless, the measurements of stellar velocity dispersion of host galaxy are difficult in optical bands because of the presence of young stars in the host galaxy. Absorption lines in optical bands such as Mg b at 517 nm and Ca triplet at 850 nm are diluted by continuum. Therefore, it is necessary to use stellar lines in other wavebands in measuring velocity dispersion. CO bandheads in near-infrared (NIR) have been suggested to be the best in studying the velocity dispersion of nearby galaxies (McConnell et al., 2011). In addition, NIR stellar lines have the potential of

* Corresponding author. Tel.: +82 312013813; fax: +82 312048122.

E-mail addresses: huynhanh7@khu.ac.kr (H.A.N. Le), soojong@khu.ac.kr (S. Pak).

Table 1
Observation log.

Date (UT)	Quasars	z	R	Echelle setting	Slit width (arcsec)	Total exposure (sec)
2003 Feb 11	PG 0844 + 349	0.064	10,000	$H+$	0.3	37×180
2004 April 3	PG 0844 + 349	0.064	5000	$H-$	0.6	10×300
2004 April 3	PG 1226 + 023	0.158	5000	$H-$	0.6	8×300
2004 April 3	PG 1226 + 023	0.158	5000	$H+$	0.6	8×300
2004 April 3	PG 1426 + 015	0.086	5000	$H-$	0.6	5×300
2004 April 3	PG 1426 + 015	0.086	5000	$H+$	0.6	5×300
2004 April 4	PG 0844 + 349	0.064	5000	$H+$	0.6	8×300
2004 April 4	PG 1426 + 015	0.086	5000	$H-$	0.6	12×300
2004 April 4	PG 1426 + 015	0.086	5000	$H+$	0.6	15×300

explaining for the relation between supermassive black holes and their host galaxies.

In this paper, we present the medium resolution host galaxy spectra of nearby quasars in H-band obtained at the Subaru telescope. Thanks to the advantages of using adaptive optics technology, we can isolate the quasar spectra from the host galaxy spectra. The obtained spectra with medium resolution can be used to determine the stellar velocity dispersions in the bulge of the host galaxies, and to estimate the supermassive black hole masses.

Section 2 of this paper shows the observation processes. The detailed data reduction processes of NIR quasar spectra are presented in Section 3. Results and discussions are shown in Section 4. Section 5 is the conclusion.

2. Observations

The observations were performed at the Subaru 8.2 m telescope using the IRCS (Kobayashi, 2000) operated with the Adaptive Optics (AO), AO36 (Hayano et al., 2008), on 2003 February 11 and 2004 April 3 and 4. The average AO-assisted point spread function was 0.3 arcsec.

2.1. Observation of quasars

We observed three nearby quasars, PG 0844 + 349, PG 1226 + 023, and PG 1426 + 015. Table 1 shows the log of the observations. In 2003, we observed PG 0844 + 349 only. The slit width was 0.3 arcsec with $R = 10^4$, and the position angle of the slit was 0 deg. The echelle setting of the spectrograph was in $H+$ setting (1.47–1.82 μm), and the total integration time was about two hours with each exposure of 180 s. The observations were done in an *Nod-off-slit* mode. We first observed the target and then moved the telescope to the nearby background sky. The sequences of the observations were *object* \rightarrow *sky* \rightarrow *sky* \rightarrow *object*.

In 2004, we observed three targets: PG 0844 + 349, PG 1226 + 023, and PG 1426 + 015. The slit width was 0.6 arcsec with $R = 5 \times 10^3$. The echelle settings of the spectrograph were in $H-$ setting (1.46–1.83 μm) and $H+$ setting, and the total integration time was one hour for each target.

Other instrument settings and the observation modes were the same as in 2003.

2.2. Standard stars and template stars

We observed A0 V type standard stars to correct the telluric absorption lines in the target spectra. In addition, bright template stars ($H < 5$ mag) in spectral classes of G, K, and M with the luminosity class of III are used to measure the velocity dispersions of the host galaxies.

3. Data reduction

Data reduction was done by using *IRAF*¹ tasks following the methods described in Pyo (2002). The details of the data reduction for standard stars and template stars can be found in Le et al. (2011). The host galaxy spectra were reduced by using similar procedures as that of the template stars. Fig. 1 shows the detailed data reduction processes.

The host galaxy spectra within the radius from 0.24 to 1.89 arcsec are extracted for PG 0844 + 039, and from 0.24 to 2.34 arcsec for PG 1226 + 023 and PG 1426 + 015. We chose the minimum radius to be 0.24 arcsec to ensure that the extracted host galaxy spectra are not affected by emission from QSOs. We confined the maximum radius to extract the host galaxy spectra within the effective radii (Peng et al., 2002) of the targets. In the case of PG 0844 + 349, the maximum radius is equal to the effective radius, $R_e = 1.89$ arcsec. The slit length² of Subaru/IRCS, $L = 5.17$ arcsec, however, is shorter than the diameters of PG 1226 + 023 ($D = 12.56$ arcsec) and of PG 1426 + 015 ($D = 8.22$ arcsec). Therefore, the maximum radius to be extracted should be smaller than half of the slit length, $L = 2.59$ arcsec.

The effects of the residual OH sky-lines could cause one of the problems of our obtained spectra. The emission lines of OH cannot be completely corrected by the sky-background subtraction processes. We masked out the data points which contain noises from the OH sky-lines.

¹ *IRAF* (Image Reduction and Analysis Facility) is distributed by the National Optical Astronomy Observatories (NOAO).

² <http://www.naoj.org/Observing/Instruments>.

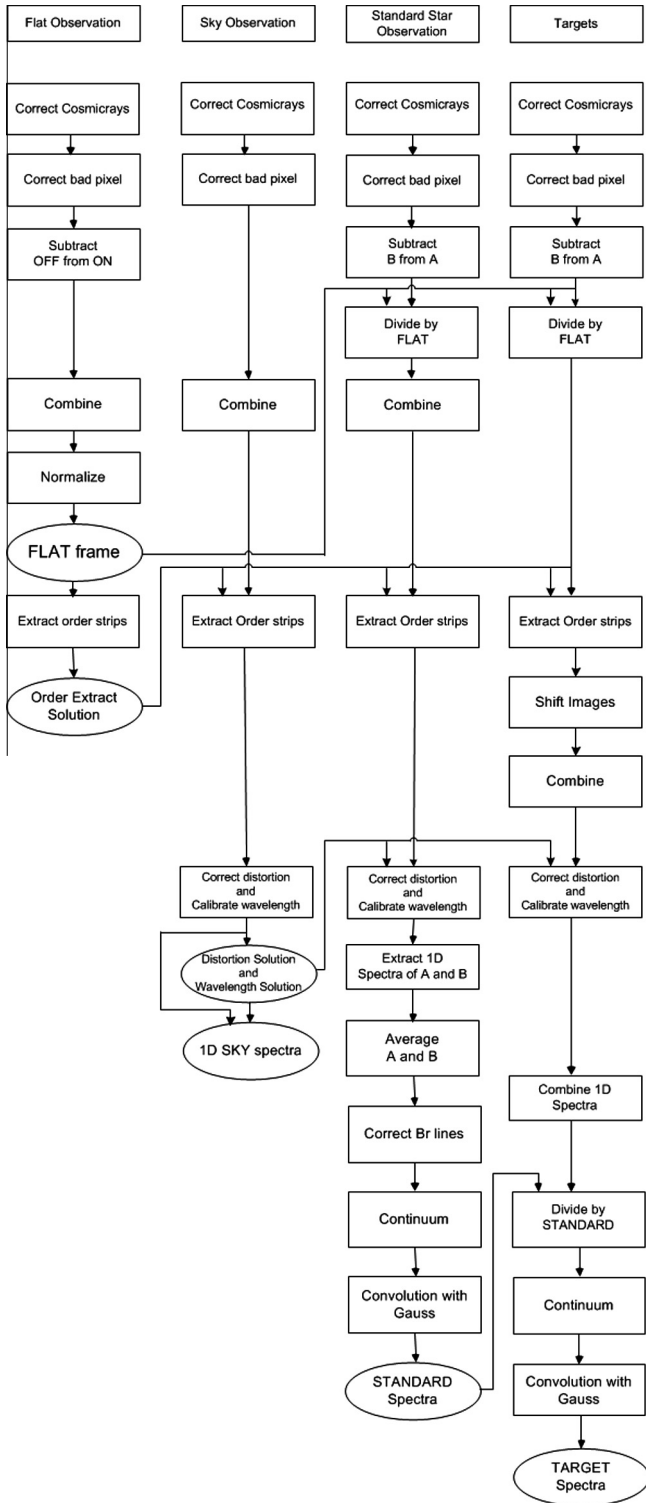


Fig. 1. Data reduction processes.

4. Results and discussion

4.1. The host galaxy spectra

Fig. 2 shows the reduced spectra of PG 0844 + 349, PG 1226 + 023, and PG 1426 + 015. In the figure, the spectrum

of K2 III (HD52071) is also plotted to be compared with the observed host galaxy spectra. In addition, the spectra of PG 1426 + 015 in Watson et al. (2008) and Dasyra et al. (2007) are shown in the figure for comparisons.

From Fig. 2, we identify prominent features, e.g., Mg I (1.488 μm), Mg I (1.503 μm), Si I (1.589 μm), and CO (6-3) (1.619 μm) in the spectrum of PG 0844 + 349. But the absorption features such as CO (3-0) (1.558 μm) and CO (4-1) (1.578 μm) cannot be seen due to the effects of the remaining OH sky-lines.

After the redshift correction, the host galaxy spectrum of PG 1226 + 023 in Fig. 2 has a limited wavelength coverage to be compared with the molecular lines of the stellar template spectrum. Unfortunately, these are not stellar spectra in the literature that overlap with the observed spectrum of PG 1226 + 023 to identify the molecular lines.

In the case of PG 1426 + 015 spectrum, we could detect Mg I (1.503 μm), Si I (1.589 μm) and CO (6-3) (1.619 μm) lines comparing the K2 III stellar template spectrum and the host galaxy spectra of Watson et al. (2008) and Dasyra et al. (2007). But the CO (3-0) (1.558 μm) and CO (4-1) (1.578 μm) lines are hard to confirm because of the effects of the remaining OH sky-lines. The signal-to-noise (S/N) ratios of Mg I and Si I absorption lines are 3. The S/N ratio of CO (6-3) absorption line is 5.

4.2. Velocity dispersion

From the obtained spectra, we identified a few stellar absorption lines of the host galaxy and measured the velocity dispersion of the host galaxy using the direct fitting method of Barth et al. (2002).

We assume that the host galaxy spectrum follows that of K2 III type stars. We define the model of host galaxy spectrum from the equation as

$$M(\lambda) = A + T_G(\lambda, \sigma) \quad (1)$$

where A is arbitrary constant value from the unknown contribution from the quasar continuum; T_G is convolution of the stellar spectrum with the line-of-sight velocity distribution; σ is the velocity dispersion; and λ is the rest wavelength. The best-fit convolved stellar spectrum to the host galaxy spectrum is found based on the minimum of chi-square values. The chi-square value is calculated by

$$\chi^2 = \sum_{\lambda} \left(\frac{M_{\lambda} - O_{\lambda}}{\epsilon_{\lambda}} \right)^2 \quad (2)$$

where M_{λ} is the model spectrum from the Eq. (1); O_{λ} is the observed host galaxy spectrum; and ϵ_{λ} is the error of the host galaxy spectrum which has typical value of 0.037 and is determined by adding the standard deviation of the spectrum to the root-mean-square of each data point.

From Fig. 2, due to the redshift correction, we could not measure the velocity dispersion of host galaxy spectrum of PG 1226 + 023. In case of PG 0844 + 349, we identified some prominent features since the effects of the remaining

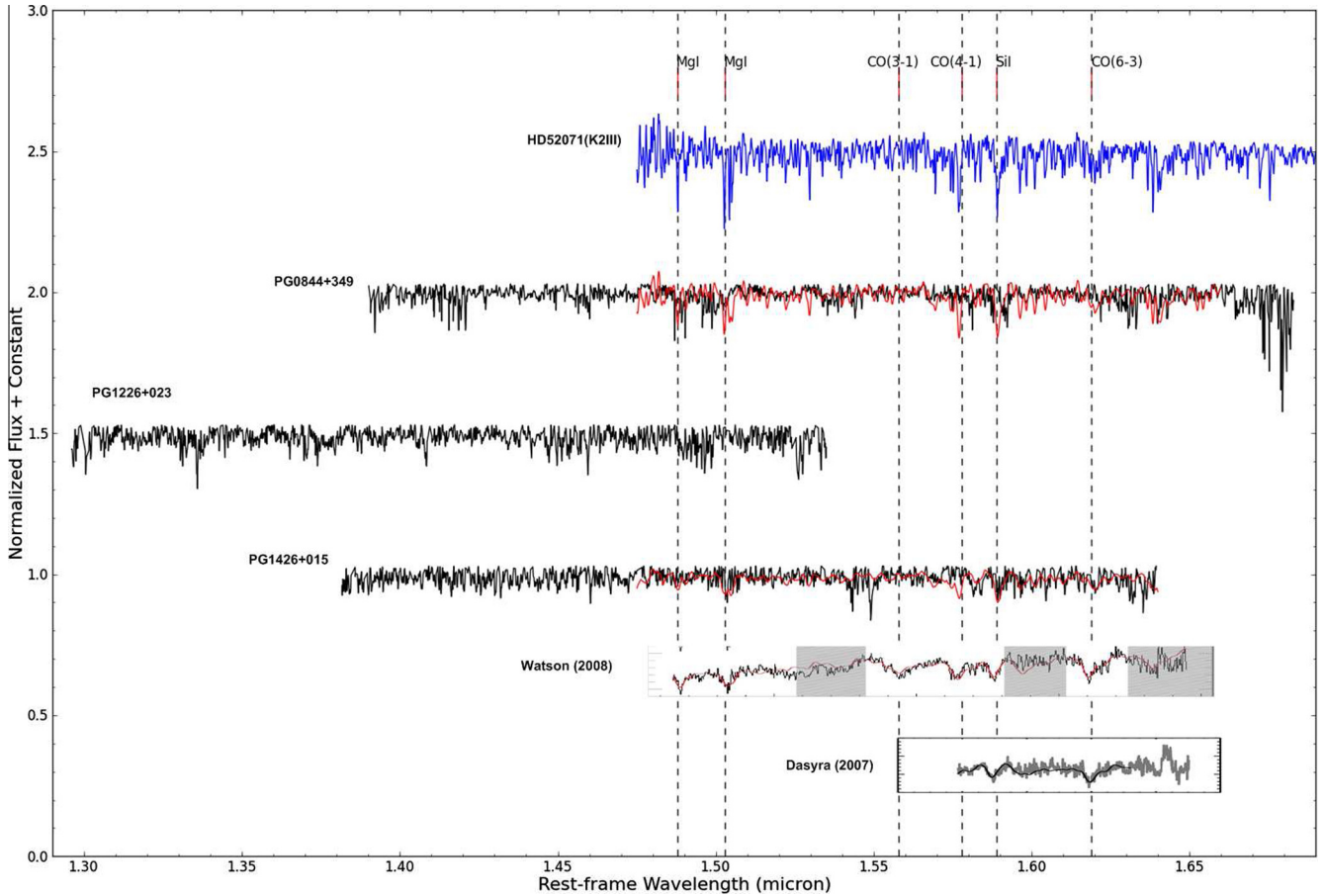


Fig. 2. Spectra of host galaxy PG 0844 + 349 (shifted with $z = 0.064$), PG 1226 + 023 (shifted with $z = 0.158$), PG 1426 + 015 (shifted with $z = 0.086$), and spectrum of K2 III (HD52071, blue-line). The red-lines show the best fit stellar spectra of K2 III (HD52071). Two spectra at the bottom show the spectra of PG 1426 + 015 from [Watson et al. \(2008\)](#) and [Dasyra et al. \(2007\)](#). (For interpretation of the references to color in this figure legend, the reader is referred to the web version of this article.)

OH sky-lines make it hard to calculate the velocity dispersion of the host galaxy. We have corrected the remaining OH sky-lines effects by removing those data points of the host galaxy spectra which are affected by sky-lines. We have calculated the velocity dispersion of the host galaxy PG 1426 + 015 to be $\sigma = 264 \pm 215 \text{ km s}^{-1}$ from the fitting with K2 III stellar spectrum at Mg I (1.503 μm) line ([Fig. 3](#)) and Si I (1.589 μm) line ([Fig. 4](#)). The reduced chi-square value is 0.8. In [Fig. 5](#), from the measurement of CO (6-3) (1.619 μm), the velocity dispersion of PG 0844 + 349 is $132 \pm 110 \text{ km s}^{-1}$ with the reduced chi-square of 0.4. Due to the low S/N ratio of the data, the errors of velocity dispersions are very large. But the best-fit sigma values which are calculated from our method are consistent with others. From the measurements of [Watson et al. \(2008\)](#) and [Dasyra et al. \(2007\)](#), the velocity dispersions of host galaxy of PG 1426 + 015 are $217 \pm 15 \text{ km s}^{-1}$ and $185 \pm 67 \text{ km s}^{-1}$, respectively, which are similar to our results. The data obtained by ISAAC long-slit spectrometer on the 8 m Antu unit of the Very Large Telescope ([Dasyra et al., 2007](#)) has higher S/N ratio compared to our data obtained by IRCS, Subaru telescope.

From the velocity dispersion measurements, we derived the black hole masses using the $M_{\text{BH}}-\sigma$ relation of elliptical galaxies ([Kormendy and Ho, 2013](#)). [Table 2](#) shows the measured values of velocity dispersion and black hole mass estimates of these quasars. The obtained black hole masses of PG 0844 + 349 and PG 1426 + 015 are $\log(M_{\text{BH}}/M_{\odot}) = 7.7 \pm 5.5$ and $\log(M_{\text{BH}}/M_{\odot}) = 9.0 \pm 7.5$, respectively.

Independently, the BH mass can be determined by using the velocity width of a broad emission line and the broad line region size from the reverberation mapping method ([Kaspi et al., 2000](#)), or the continuum/line luminosity ([Kim et al., 2010](#)). Assuming a virial factor of $f = 5.5$ in [Onken et al. \(2004\)](#) and [Woo et al. \(2013\)](#); [Peterson et al. \(2004\)](#) find that the BH masses are $\log(M_{\text{BH}}/M_{\odot}) = 8.0 \pm 0.2$ for PG 0844 + 349 and $\log(M_{\text{BH}}/M_{\odot}) = 9.1 \pm 0.2$ for PG 1426 + 015.

5. Conclusions

We obtained NIR medium resolution host galaxy spectra of nearby quasars, PG 0844 + 349, PG 1226 + 023, and PG 1426 + 015 in H-band, using the IRCS instrument and

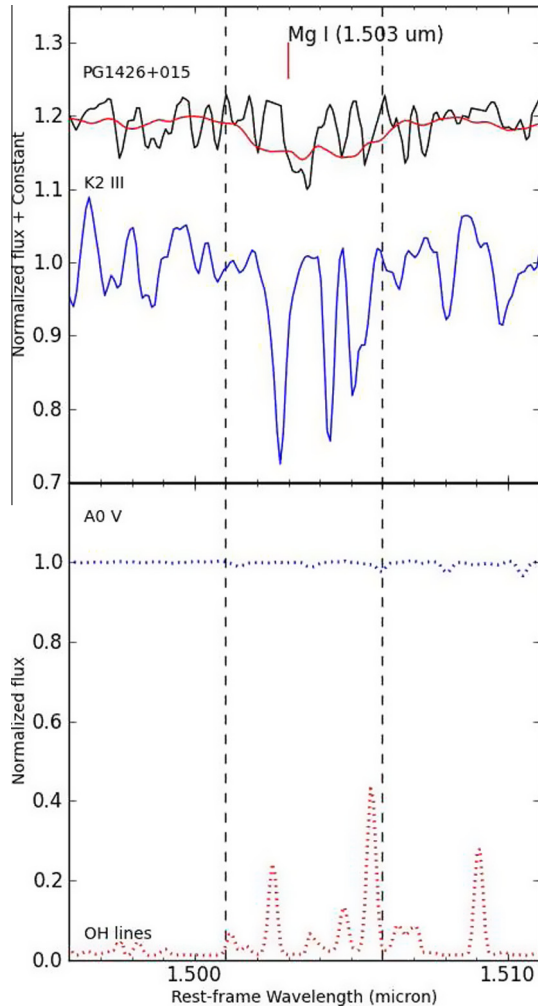


Fig. 3. Spectra of K2 III (HD52071) (blue-line) and host galaxy PG 1426 + 015 (shifted with $z = 0.086$) (black-line). The best fit of the velocity convolved K2 III spectrum is shown in red-line. The dashed lines show the regions used for measurements of velocity dispersions. The A0 V and OH sky-lines spectra are shown in the lower plot. (For interpretation of the references to color in this figure legend, the reader is referred to the web version of this article.)

the AO of the Subaru telescope. The data analysis method of the NIR spectra is presented.

From the spectra, we derived the stellar velocity dispersion of the host galaxy and its relation to the central supermassive BH. From the identified stellar absorption lines, we have obtained the velocity dispersion of PG 1426 + 015 to be $264 \pm 215 \text{ km s}^{-1}$ based on the measurement of Mg I (1.503 μm) and Si I (1.589 μm). In the case of PG 0844 + 349, we have measured the velocity dispersion of the host galaxy to be $132 \pm 110 \text{ km s}^{-1}$ based on the calculation of CO (6-3) (1.619 μm).

By using an $M_{\text{BH}}-\sigma$ relation of elliptical galaxies, the BH masses of PG 0844 + 349 and PG 1426 + 015 are estimated to be $\log(M_{\text{BH}}/M_{\odot}) = 7.7 \pm 5.5$ and $\log(M_{\text{BH}}/M_{\odot}) =$

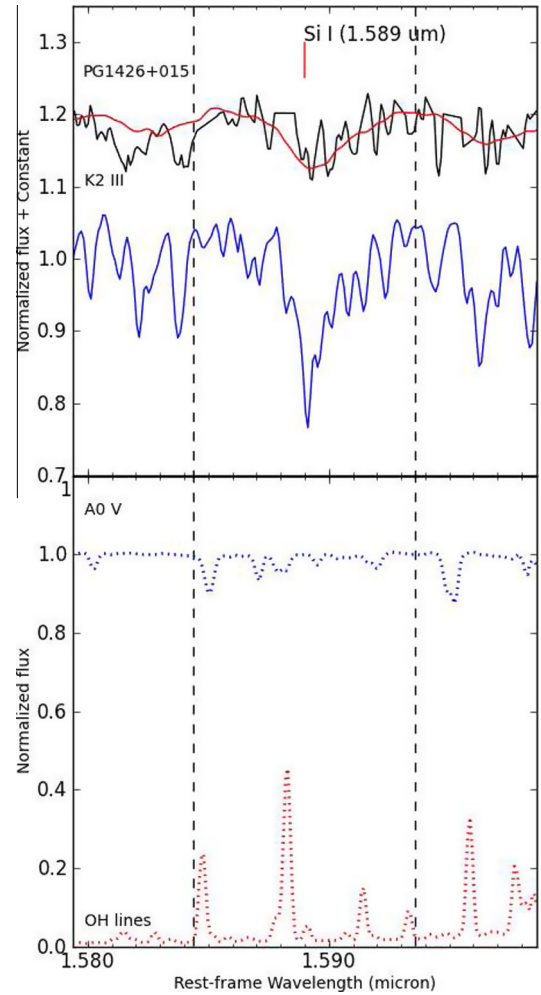


Fig. 4. Spectra of K2 III (HD52071) (blue-line) and host galaxy PG 1426 + 015 (shifted with $z = 0.086$) (black-line). The best fit of the velocity convolved K2 III spectrum is shown in red-line. The dashed lines show the regions used for measurements of velocity dispersions. The A0 V and OH sky-lines spectra are shown in the lower plot. (For interpretation of the references to color in this figure legend, the reader is referred to the web version of this article.)

9.0 ± 7.5 , respectively. These values are consistent with the BH masses from the quasar broad emission lines.

Acknowledgement

This work was supported by the National Research Foundation of Korea (NRF) grant, No. 2008-0060544, funded by the Korea government (MSIP). We appreciate Tae-Soo Pyo and Hiroshi Terada for observations and data reductions, and Elaine S. Pak for proofreading this manuscript. LCH acknowledges support from the Chinese Academy of Science through grant No. XDB09030102 (Emergence of Cosmological Structures) from the Strategic Priority Research Program. This work is based on the data collected at Subaru Telescope, which is operated by the National Astronomical Observatory of Japan.

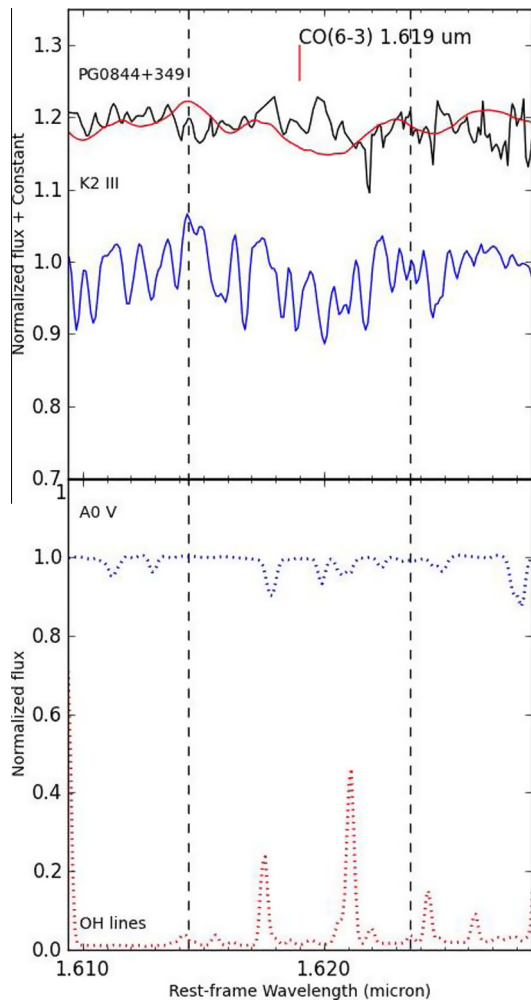


Fig. 5. Spectra of K2 III (HD52071) (blue-line) and spectra of host galaxy PG 0844 + 349 (shifted with $z = 0.064$). The best fit of the velocity convolved K2 III spectrum is shown in red-line. The dashed lines show the regions used for measurements of velocity dispersions. The A0 V and OH sky-lines spectra are shown in the lower plot. (For interpretation of the references to color in this figure legend, the reader is referred to the web version of this article.)

Table 2
Velocity dispersion measurements and black hole masses.

Quasars	σ^a (km s $^{-1}$)	σ^b (km s $^{-1}$)	$\log (M_{\text{BH}}/M_{\odot})^c$	$\log (M_{\text{BH}}/M_{\odot})^d$
PG 0844 + 349	132 ± 110^e		7.7 ± 5.5	8.0 ± 0.2
PG 1426 + 015	264 ± 215^f	217 ± 15	9.0 ± 7.5	9.1 ± 0.2

^a This work.

^b Velocity dispersion values from Watson et al. (2008).

^c This work. Black hole mass values are derived by using the formula (7) of Kormendy and Ho (2013).

^d Black hole mass values from Peterson et al. (2004).

^e Velocity dispersion value based on the measurement of CO (6-3) (1.619 μm) line.

^f Velocity dispersion value based on the measurements of Mg I (1.508 μm) and Si I (1.589 μm) lines.

References

- Barth, A.J., Ho, L.C., Sargent, W.L.W., 2002. A study of the direct fitting method for measurement of galaxy velocity dispersions. *AJ* 124, 2607.
- Dasyra, K.M., Tacconi, L.J., Davies, I.R., Genzel, R., Lutz, D., Peterson, B.M., Veilleux, S., Baker, A.J., Schweitzer, M., Sturm, E., 2007. Host dynamics and origin of Palomar–Green QSOs. *ApJ* 657, 102.
- Ferrarese, L., Pogge, R.W., Peterson, B.M., Merritt, D., Wandel, A., Joseph, C.L., 2001. Supermassive black holes in active galactic nuclei. I. The consistency of black hole masses in quiescent and active galaxies. *ApJ* 555, L79.
- Gebhardt, K., Kormendy, J., Ho, L.C., et al., 2000a. A relationship between nuclear black hole mass and galaxy velocity dispersion. *ApJL* 539, L13.
- Gebhardt, K., Bender, R., Bower, G., et al., 2000b. Black hole mass estimates from reverberation mapping and from spatially resolved kinematics. *ApJL* 543, L5.
- Hayano, Y., Takami, H., Guyon, O., Oya, S., Hattori, M., Saito, Y., Watanabe, M., Murakami, N., Minowa, Y., Ito, M., Colley, S., Eldred, M., Golota, G., Dinkins, M., Kashikawa, N., Iye, M., 2008. Current status of the laser guide star adaptive optics system for Subaru telescope. *Proc. SPIE* 7015, 701510.
- Kaspi, S., Smith, P.S., Netzer, H., Maoz, D., Jannuzi, B.T., Giveon, U., 2000. Reverberation measurements for 17 quasars and the size–mass–luminosity relations in active galactic nuclei. *ApJ* 533, 631.
- Kim, D., Im, M., Kim, M., 2010. New estimators of black hole mass in active galactic nuclei with hydrogen Paschen lines. *ApJ* 724, 386.
- Kobayashi, N. et al., 2000. IRCS: infrared camera and spectrograph for the Subaru telescope. *SPIE* 4008, 1056.
- Kormendy, J., Ho, L.C., 2013. Coevolution (or not) of supermassive black holes and host galaxies. *ARAA* 51, 511.
- Le, H.A.N., Kang, W., Pak, S., Im, M., Lee, J.E., Ho, L.C., Pyo, T.S., Jaffe, D.T., 2011. Medium resolution spectral library of late-type stellar templates in near-infrared band. *JKAS* 44, 125.
- McConnell, N.J. et al., 2011. The black hole mass in brightest cluster galaxy NGC 6086. *AJ* 728, 100.
- Onken, C.A., Ferrarese, L., Merritt, D., Peterson, B.M., Pogge, R.W., Vestergaard, M., Wandel, A., 2004. Supermassive black holes in active galactic nuclei. II. Calibration of the black hole mass–velocity dispersion relationship for active galactic nuclei. *ApJ* 615, 645.
- Peng, C.Y., Ho, L.C., Impey, C.D., Rix, H.W., 2002. Detailed structural decomposition of galaxy images. *AJ* 124, 266.
- Peterson, B.M., Ferrarese, L., Gilbert, K.M., et al., 2004. Central masses and broad-line region sizes of active galactic nuclei. II. A homogeneous analysis of a large reverberation-mapping database. *ApJ* 613, 682.
- Pyo, T.S., 2002. Near Infrared [Fe II] Spectroscopy of Jets and Winds Emanating from Young Stellar Objects (Ph.D. thesis). Tokyo Univ.
- Richstone, D. et al., 1998. Supermassive black holes then and now. *Nature* 395, A14.
- Watson, L.C., Martini, P., Dasyra, K.M., Bentz, M.C., Ferrarese, L., Peterson, B.M., Pogge, R.W., Tacconi, L.J., 2008. First stellar velocity dispersion measurement of a luminous QSO host with Gemini North laser guide star adaptive optics. *ApJ* 682, L21.
- Woo, J.H., Schulze, A., Park, D., Kang, W.R., Kim, S.C., Riechers, D.A., 2013. Do quiescent and active galaxies have different $M_{\text{BH}}-\sigma_*$ relations? *ApJ* 772, 49.